Conductivity and Structural Studies of Poly(vinylidene fluoride co-hexafluoropropylene)/Polyethyl methacrylate Blend Doped with Ammonium Triflate

S. Rudzhiah[1], N.S. Mohamed[2], A. Ahmad[3,]*

[1] Center for Foundation Studies, Universiti Tekhnologi MARA, 42300 Bandar Puncak Alam, Selangor, Malaysia
[2] Center for Foundation Studies in Science, University of Malaya, 50603 Kuala Lumpur, Malaysia.
[3] School of Chemical Science and Food Technology, Faculty of Science and Technology, Universiti Kebangsaan Malaysia, 43600 Bangi Selangor Malaysia.
[*]E-mail: azizan@ukm.my

Flexible free standing of Poly(vinylidene fluoride co-hexafluoropropylene)/Polyethyl methacrylate-amonium triflate electrolyte systems have been successfully prepared using solution casting technique. The prepared films were characterized using X-ray diffraction, scanning electron microscopy, differential scanning calorimetry, impedance spectroscopy and ionic transference number measurements in order to investigate their structural, thermal, electrical and electrochemical properties. The conductivity is observed to increase with increasing ammonium triflate concentration. The film of electrolyte containing 40 wt % of salt exhibited optimum room temperature conductivity of 7.07×10^{-4} S cm^{-1}. The increase in the conductivity is attributed to the increase in the number of ions as the salt concentration is increased. This has been proven by dielectric studies. The increase in conductivity is also attributable to the increase in the fraction of amorphous region in the electrolyte films as confirmed by X-ray diffraction and differential scanning calorimetric studies.

1. INTRODUCTION

Blending of polymers is an economical technique to develop new polymeric materials with properties that are superior, intermediate, or just different from those of individual component polymers. Polymer blends have received great interest in recent years due to its advantages including simplicity of preparation. An additional advantage is ease of control of properties by changing the component polymers and their compositions. It has been reported that the polymer electrolytes developed using polymer blends exhibited higher conductivity [1,2] and better mechanical strength

[3-5] compared to the electrolytes based on pure polymer. The enhancement of conductivity has been attributed to the increase in amorphous region in the blend based electrolytes.

Polymer blends containing poly(vinylidene fluoride co-hexafluoropropylene) (PVDF-HFP) have been used as host polymers for polymers for polymer electrolytes by a few group of researchers [3,6,7]. Michael and Prabharan [6] studied the conductivity of PVDF-HFP/PVK blend based electrolytes. They reported that the ionic conductivity of PVDF-HFP-1.5MLiBF$_4$/EC without PVK exhibited high conductivity 0.16×10^{-3} S cm^{-1} at room temperature but mechanical strength of the polymer films was obviously poor. This problem was overcome by the addition of PVK which increased the conductivity ~4.5 times higher (0.72×10^{-3} S cm^{-1}). In addition, PVK also enhanced the mechanical strength of PVDF-HFP based electrolytes. Other researchers had prepared PVDF-HFP/PHEMO-LiTFSi electrolytes by solution casting technique [7]. They reported that the conductivity of the polymer electrolytes reached 1.64×10^{-4} S cm^{-1} at 30 $^{\circ}$C. They reported that their PVDF-HFP/PHEMO polymer electrolyte has good electrochemical stability and thermal stability. Fan and co-workers [3] reported their studies on thermal, electrical and mechanical properties of polymer electrolytes based on PEO blended with PVDF-HFP. A good combination between high ionic conductivity and mechanical stability were obtained from PEO/PVDF-HFP based polymer electrolytes.

PVDF-HFP is one of the polymer hosts that attracted the attention of many groups of researchers due to its unique characteristics. However, PVDF-HFP alone forms brittle films. In the present work, PVDF-HFP was blended with polyethyl methacrylate (PEMA) to improve this brittle property and hence more flexible films can be obtained. PEMA was chosen as it is an amorphous polymer [8] and contains carbonyl group in its structure that may provide additional coordinating sites for ions of the doping salt [2]. This study also investigated the characteristics of PVDF-HFP/PEMA electrolyte films based on this PVDF-HFP/PEMA blend.

2. MATERIAL AND METHODS

2.1 Preparation of Materials

The PVDF-HFP (M$_w$~400, 000)/PEMA (M$_w$~515,000)-ammonium triflate (NH$_4$CF$_3$SO$_3$) (99%, Aldrich) electrolyte films were prepared by adding different weight percentages of NH$_4$CF$_3$SO$_3$ to solutions containing fixed amounts of PVDF-HFP and PEMA. The weight percentage of salt was calculated using the equation:

$$wt_{salt} \% = \frac{wt_{salt}}{wt_{PVDFHFP} + wt_{PEMA} + wt_{salt}} \times 100 \% \dots\dots\dots\dots\dots\dots\dots (1)$$

where $wt_{PVDF-HFP}$, wt_{salt} and wt_{PEMA} are the weight of salt, PVDF-HFP and PEMA respectively. The solutions were stirred at 40 $^{\circ}$C for 48 hours and poured into Petri dishes and left to evaporate slowly to form films.

2.2 Characterization of materials

        In order to study the crystalline nature of polymer electrolyte films studied in this work, X-ray diffraction was performed. The XRD patterns of the polymer systems were recorded using D8 Advanced X-Diffractometer Bruker AXS in the 2θ range from 3° to 80°. Surface morphology was carried out using LEICA 5000 Scanning Electron Microscope. The samples were examined under a vacuum condition. The thermal characteristics of the polymer electrolytes in this study were determined using DSC METTLER TOLEDO DSC822 under Argon condition at a scan rate of 50ml/min. Each sample was sealed in aluminum crucible and heated from -60 to 200 ^{o}C. The characterization of electrical properties of solid polymer electrolytes in this study was performed by impedance spectroscopic technique using HIOKI 3532 LCR HiTESTER in the frequency range between 42 Hz and 5 MHz at various temperatures from 303 K to 353 K. Each sample was sandwiched between stainless steel blocking electrodes of diameter 2.5 cm (area = 4.9094 cm^2). The transference number measurements were carried out using DC polarization method. In this study, the carbon/PVDF-HFP/PEMA-NH$_4$CF$_3$SO$_3$/carbon cell was polarized by applying a voltage of 1.0 V and the current was monitored.

3. RESULTS AND DISCUSSION

3.1 XRD study
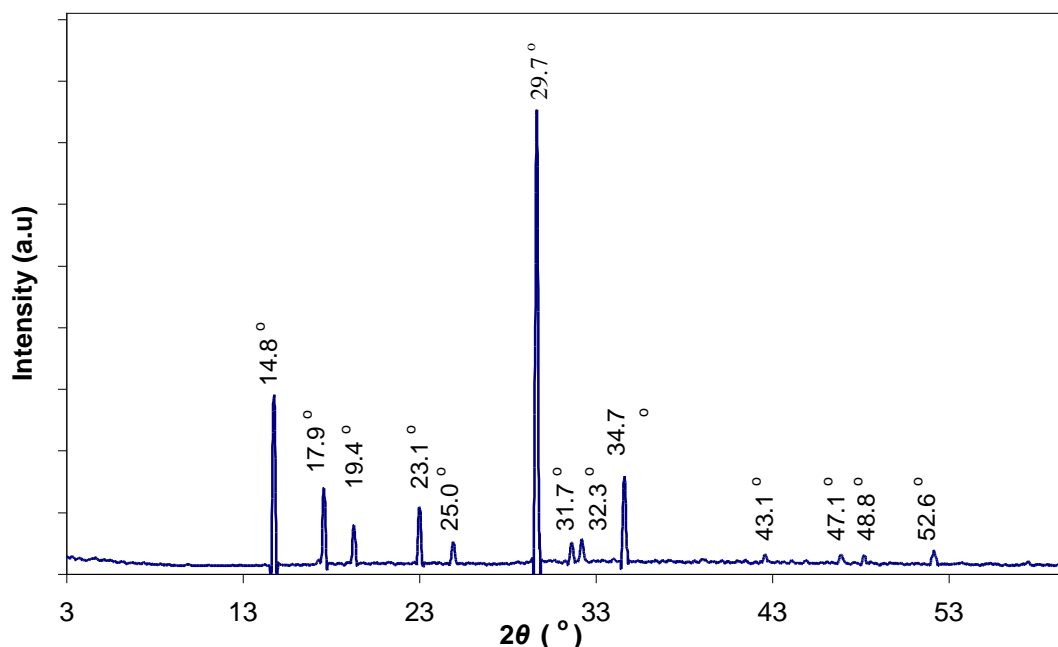
Figure 1a. X-ray diffraction pattern of NH$_4$CF$_3$SO$_3$

        X-ray diffraction pattern of NH$_4$CF$_3$SO$_3$ is illustrated in Figure 1(a). High intensity and well distinguished peaks are observed at 2θ = 14.7, 17.9, 19.4, 23.1, 25.0, 29.7, 31.7, 32.3, 34.7, 43.1, 47.1, 48.8 and 52.6^o in this spectrum. The X-ray diffraction patterns of PVDF-HFP/PEMA-NH$_4$CF$_3$SO$_3$ films with various concentrations of salt are displayed in Figure 1(b). The XRD pattern of PVDF-HFP/PEMA blend (0 wt %) film in this figure reveals peak at 2θ of 20.3^o. With addition of upto 30 wt

% of salt, the peak at $2\theta = 20.3^{\circ}$ is broadened and its intensity is reduced. This shows that the $NH_4CF_3SO_3$ salt has disrupted the crystalline region in the PVDF-HFP/PEMA blend system. Further broadening and reduction in intensity of the peak are observed with the addition of 40 wt % of $NH_4CF_3SO_3$ salt indicating an increase in the fraction of amorphous region [9,10].
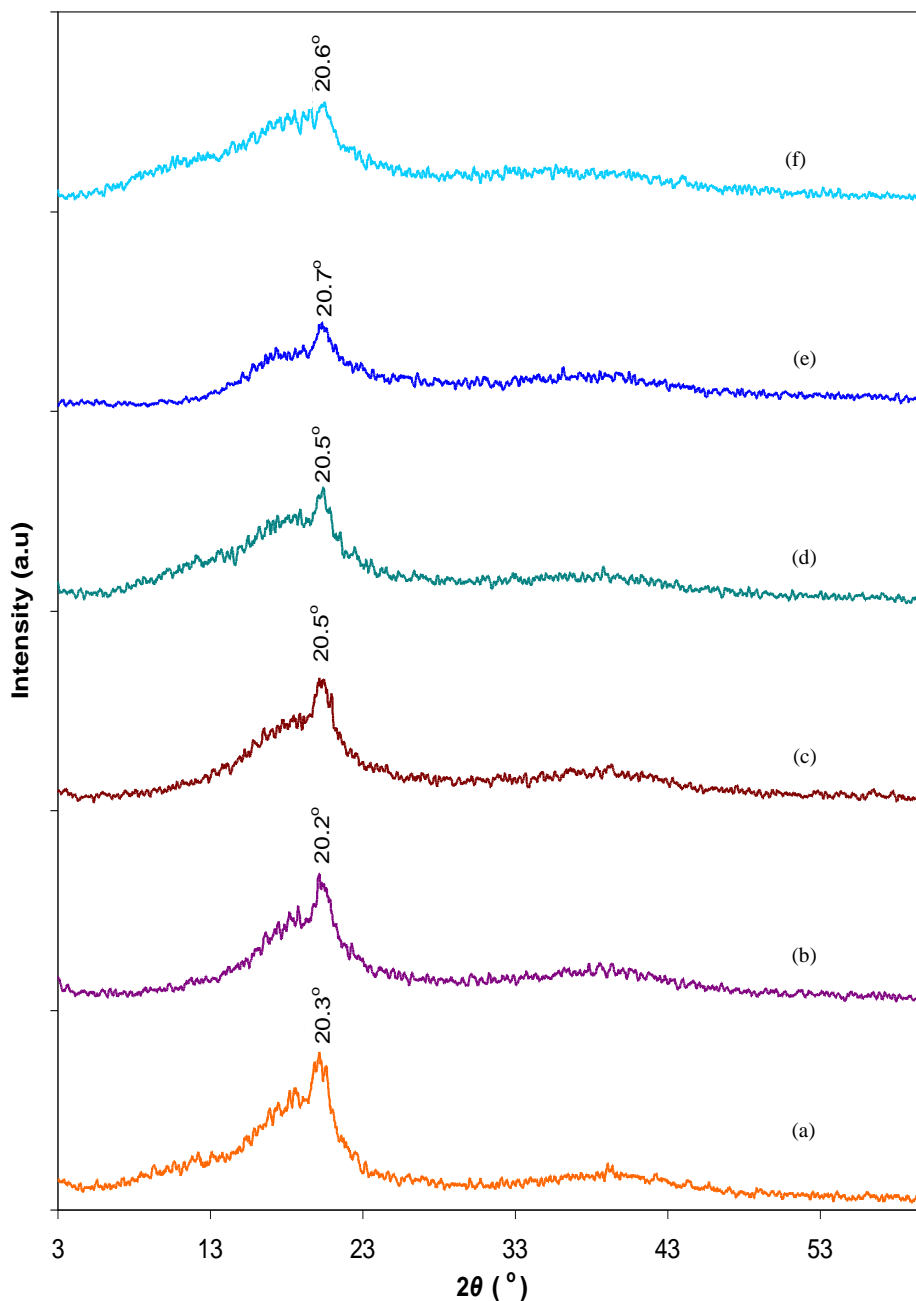
Figure 1b. X-ray diffraction patterns of films of PVDF-HFP/PEMA containing (a) 0, (b) 15, (c) 20, (d) 30, (e) 40 and (f) 45 wt % of $NH_4CF_3SO_3$

3.2 SEM Study

Figure 2 shows the surface morphology image of the film of PVDF-HFP/PEMA blend, at a magnification of 50×. The figure clearly shows that large sized spherulites are distributed quite

homogenously. The size of the spherulites (average size of 34 μm) of the unsalted PVDF-HFP/PEMA is reduced with the addition of salt. This is another evidence to show that the addition of $NH_4CF_3SO_3$ has disrupted the morphology of PVDF-HFP/PEMA blend.
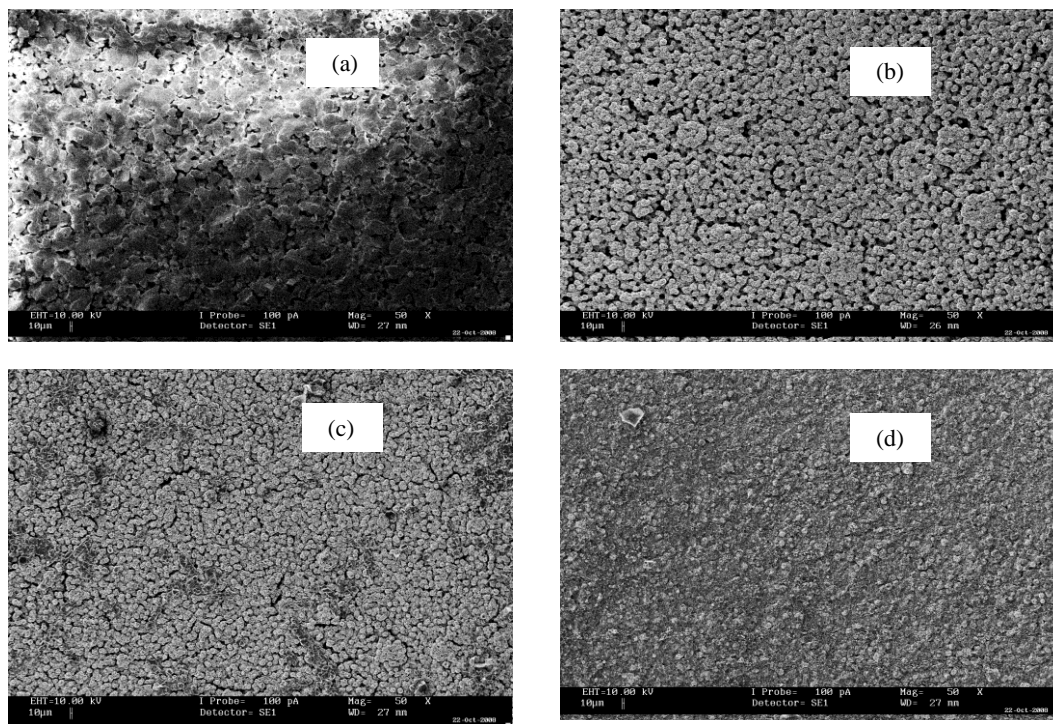
Figure 2. SEM micrographs of films of PVDF-HFP/PEMA containing (a) 0, (b) 15, (e) 40 and (f) 45 wt % of $NH_4CF_3SO_3$

3.3 DSC Study

Table 1. Melting point, melting enthalpy and relative percentage of crystallinity values for PVDF-HFP/PEMA-$NH_4CF_3SO_3$ systems

PVDF-HFP/ PEMA-(x wt %) $NH_4CF_3SO_3$	T_{m1} (^{o}C)	T_{m2} (^{o}C)	ΔH_{m1} (J g^{-1})	ΔH_{m2} (J g^{-1})	X_c (%)
10	139.2	-	13.75	-	13.13
20	139.0	164.2	8.22	0.23	8.07
25	138.0	171.0	7.48	0.96	8.06
30	138.0	165.4	6.10	1.11	6.89
40	137.4	161.2	3.44	2.12	5.31
50	138.0	160.8	4.49	1.66	5.87

Thermal properties of PVDF-HHFP/PEMA-$NH_4CF_3SO_3$ films were analyzed using DSC measurements. Figure 3 depicts the DSC curves for the films of PVDF-HFP/PEMA blend and PVDF-HFP/PEMA with different concentrations of $NH_4CF_3SO_3$ salt. The endothermic peak observed in the

temperature range 130-150 ^{o}C is ascribed to the melting point of PVDF-HFP [11]. The values of the melting temperature (T_{m1} and T_{m2}), enthalpy of melting (ΔH_{m1} and ΔH_{m2}) and relative percentage of crystallinity (X_c) are listed in Table 1. The value of melting temperature of PVDF-HFP is found to decrease with increase in salt concentration. According to Choi et al., the decrease in melting temperature was attributable to the decrease of shperulites sizes [12]. However, a second endothermic band is observed in the temperature range 160 to 170 ^{o}C in the system containing more that 10 wt% salt. This peak is associated with the melting of crystalline γ-phase PVDF [13]. The lowest melting temperature was obtained for the system containing 40 wt% of $NH_4CF_3SO_3$. The relative percentage of crystallinity, X_c of PVDF-HFP/PEMA-$NH_4CF_3SO_3$ was calculated using the following equation,

$$X_c = \frac{\Delta H_m}{\Delta H_o} \times 100\%$$ …………………………………….(1)

where ΔH_m is the melting enthalpy obtained from the DSC results. ΔH_o is the melting enthalpy of 100% crystalline PVDF-HFP which is assumed to be 104.7 J g^{-1} [13].
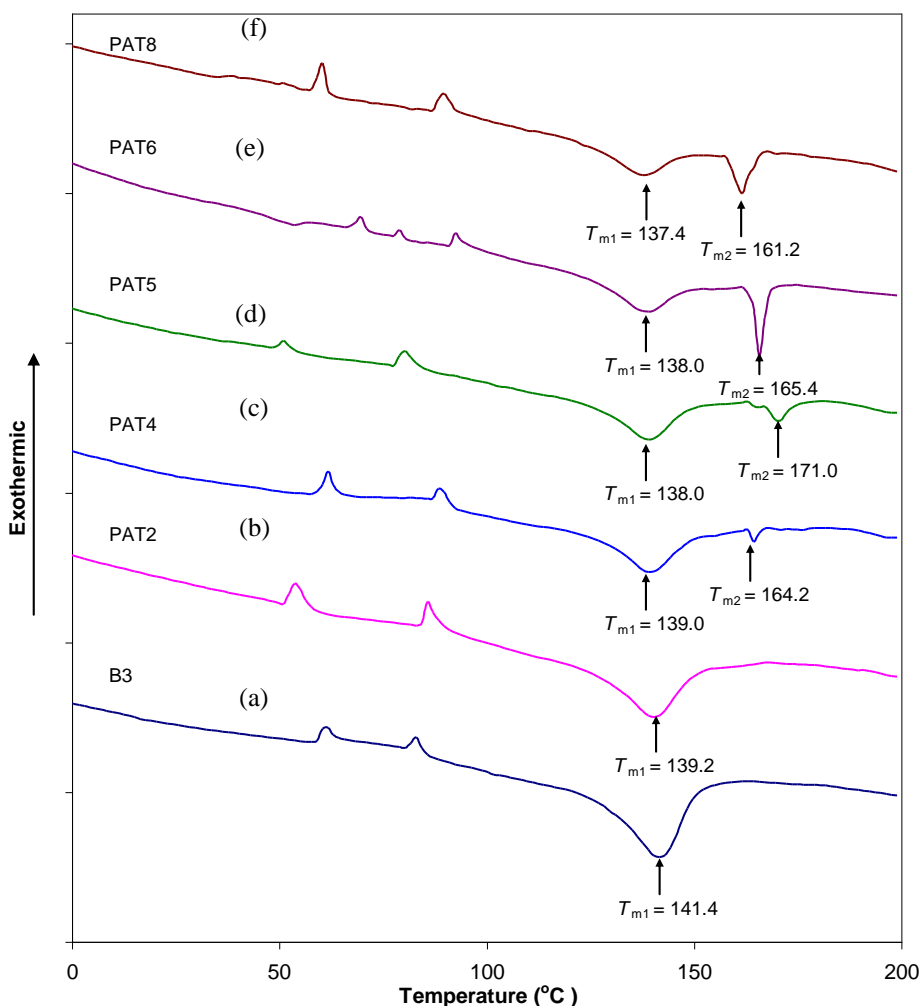
Figure 3. DSC curves for films of PVDF-HFP/PEMA containing (a) 0, (b) 10, (c) 25, (d) 30, and (e) 40 wt % of $NH_4CF_3SO_3$

It is observed that the relative percentage of crystallinity decreased from 15.11 % to 5.3 % with the increase in $NH_4CF_3SO_3$ salt concentration of from 5 to 40 wt % but it increased slightly when there was an addition of 45 wt % $NH_4CF_3SO_3$ salt. The relative percentage of crystallinity was lowest for the film containing 40 wt % salt. This means that this film is the most amorphous among the PVDF-HFP/PEMA-$NH_4CF_3SO_3$ films.

3.4 Room Temperature Conductivity Study
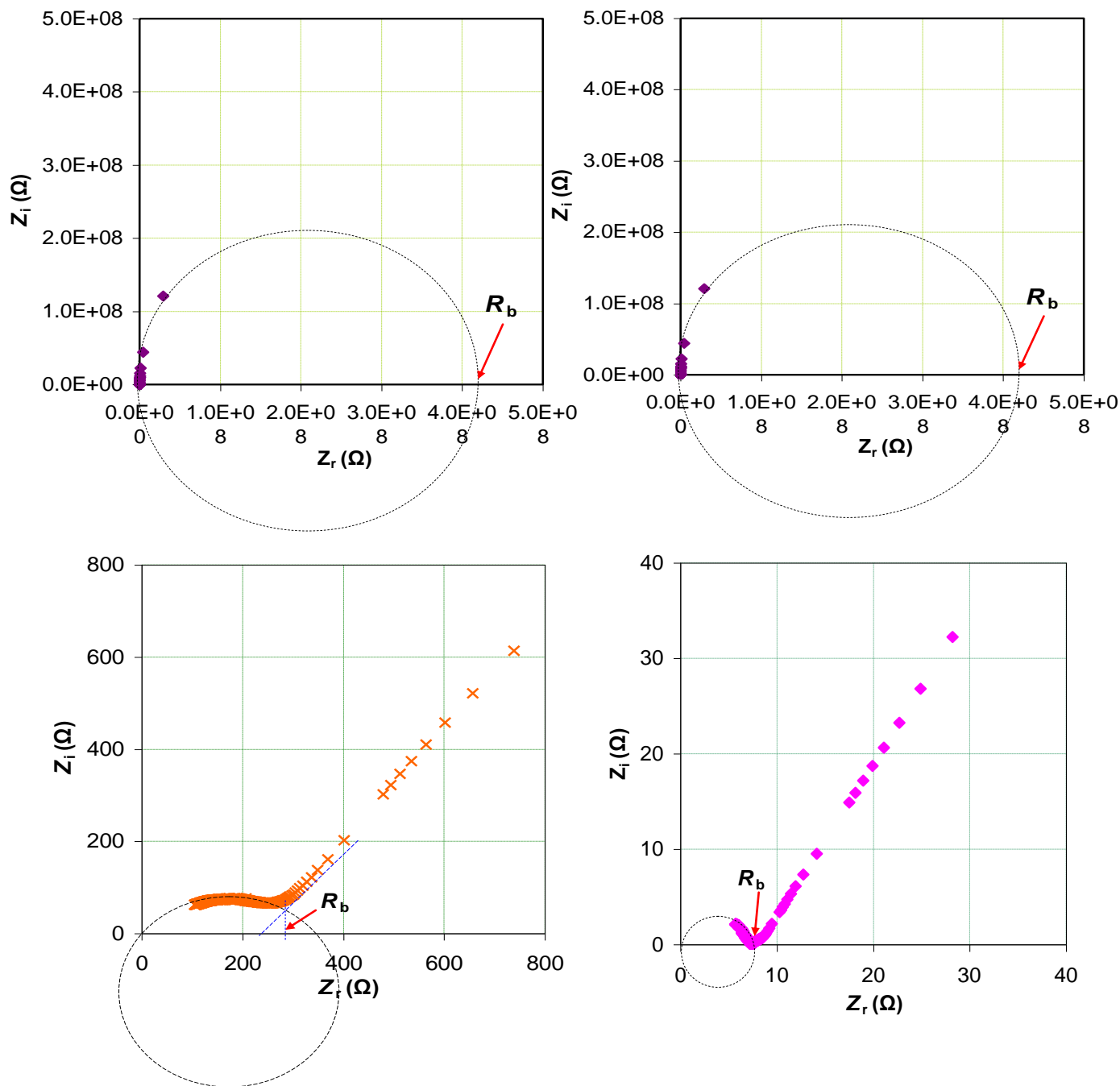
Figure 4. Impedance plots of films of PVDF-HFP/PEMA-$NH_4CF_3SO_3$ containing (a) 0, (b) 15, (c) 20, and (d) 40 wt % of $NH_4CF_3SO_3$

Figure 4 presents the impedance plots for PVDF-HFP/PEMA-$NH_4CF_3SO_3$ films containing 0, 15, 35 and 40 wt % of $NH_4CF_3SO_3$ at room temperature. The Z_i versus Z_r plot for the system containing 0 wt % $NH_4CF_3SO_3$ consisted of a small portion of a depressed semicircle while the system containing 15, 35 and 40 wt % salt plots shows an arc and a spike. The high frequency arc can be represented by a parallel combination of a constant phase element (due to the immobile polymer chains that became polarized in an alternating field) and a resistor (due to the mobile ion in the polymer matrix). The low frequency spike is attributed to the double layer response at the electrode electrolyte interface [14-16]. The bulk resistance R_b, of the system without salt was determined from the intercept of the high frequency end of the extrapolated semicircle with the Z_r axis while R_b, of the salt system was determined from the intercept of the high frequency semicircle and low frequency spike. The value of R_b is observed to decrease with increasing salt concentration. The conductivity of the samples were calculated using equation,

$$\sigma = \frac{t}{R_bA} \dots\dots\dots\dots\dots\dots\dots\dots\dots\dots\dots\dots\dots\dots\dots.(2)$$

where t is the thickness of the sample, A is the area of blocking electrode and R_b is the bulk resistance.
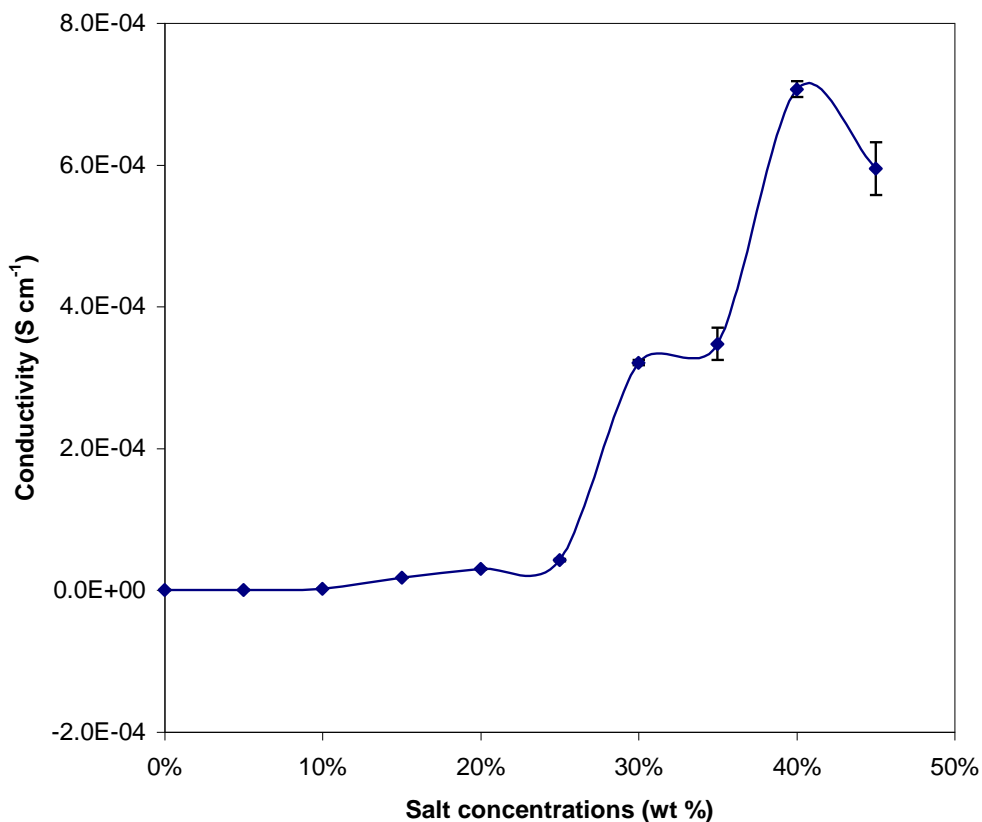
Figure 5. Plot of conductivity PVDF-HFP/PEMA-$NH_4CF_3SO_3$ versus $NH_4CF_3SO_3$ concentration

Figure 5 shows the variation of conductivity of the PVDF-HFP/PEMA-NH$_4$CF$_3$SO$_3$ films investigated in this study. Initially, upon the addition of 5 wt % of NH$_4$CF$_3$SO$_3$ the conductivity increased from 2.97×10^{-11} S cm^{-1} to 1.46×10^{-8} S cm^{-1}. With the addition of NH$_4$CF$_3$SO$_3$ from 10 to 40 wt % of salt, the conductivity of the PVDF-HFP/PEMA blend is observed to gradually increase up to four orders of magnitude. The increase in conductivity can be attributed to the increase in mobile ion concentration and the increase in the fraction of amorphous region as shown by XRD and DSC studies. However, the conductivity is observed to decrease at the salt concentration of 45 wt %. The decrease in conductivity could be assigned to the dominating role of ion association over free ion formation which decreases the number of charge carriers for conduction [17]. The polymer electrolyte film containing more than 45 wt % NH$_4$CF$_3$SO$_3$ was mechanically unstable and therefore impedance measurement was not performed on it. The PVDF-HFP/PEMA film containing 40 wt % NH$_4$CF$_3$SO$_3$ salt exhibited the highest conductivity of 7.07×10^{-4} S cm^{-1}.

3.5 Temperature Dependence of Ionic Conductivity Study

The temperature dependence of conductivity was performed in a temperature range from 30 to 75 °C in order to understand the conductivity-temperature behavior of PVDF-HFP/PEMA-NH$_4$CF$_3$SO$_3$ films. The impedance data at various temperatures were collected and analyzed.
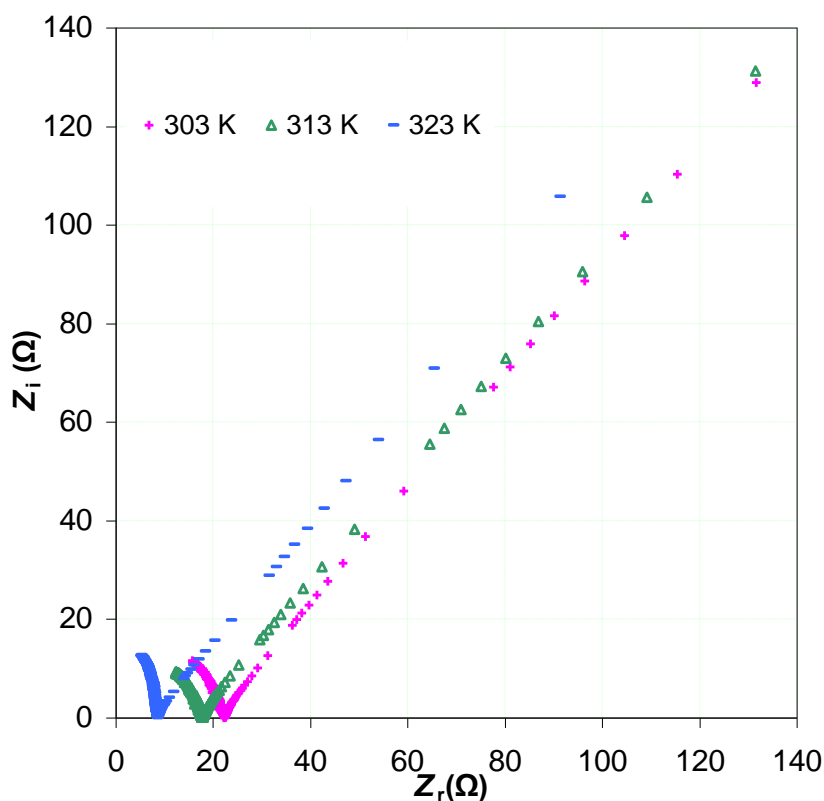
Figure 6. Impedance plots of PVDF-HFP/PEMA-NH$_4$CF$_3$SO$_3$ film containing 40 wt % of NH$_4$CF$_3$SO$_3$ at various temperatures

Figure 6 depicts the impedance plots of 40 wt % electrolyte film at various temperatures. Each impedance plot shown in this figure consists of an incomplete semicircle at low frequency regions and a spike at high frequency regions. At high temperatures the slope of the spikes are leaning towards the imaginary impedance axis which is an indication of the establishment of better contact between the electrolyte and the electrodes [18].
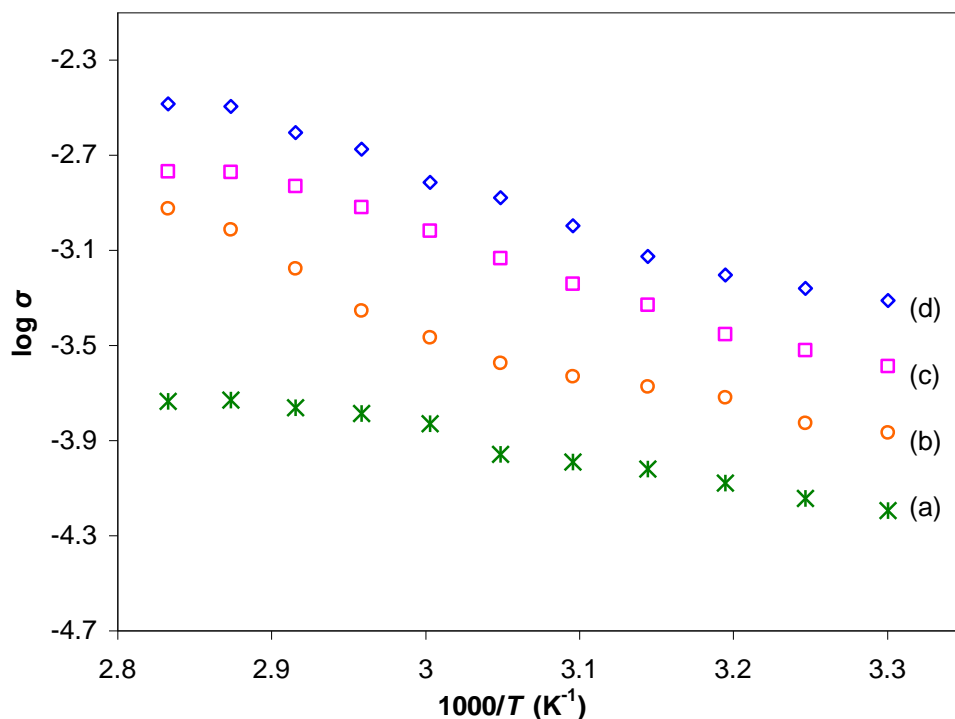
Figure 7. The Arrhenius plots of PVDF-HFP/PEMA-NH$_4$CF$_3$SO$_3$ film containing 10, 20, 35 and 40 wt % NH$_4$CF$_3$SO$_3$

Figure 7 depicts the variation of conductivity with temperature plots for polymer electrolyte films containing 10, 20, 30, 35 and 40 wt % of NH$_4$CF$_3$SO$_3$ salts respectively. The conductivity of the systems is observed to increase with the variation of temperature. However, for the polymer electrolyte films containing 10 and 20 wt % of salt, a sudden increase in the conductivity is observed at $1000/T = 3.0489$ K^{-1} ($T = 55$ ^{o}C). This is possibly due to PVDF-HFP crystalline phase transition [17].

The curvature of σ vs $1000/T$ plots suggests that ion transport in the PVDF-HFP/PEMA-NH$_4$CF$_3$SO$_3$ polymer electrolytes is dependent on host polymer segmental motion. At high temperatures, thermal movement of polymer chain segments and the dissociation of salts are improved leading to an increase in conductivity. However, at low temperatures, the presence of salt leads to salt-polymer or cation-dipole interaction, which increases the cohesive energy of polymer networks. As the free volume decreases, polymer segmental motion and ionic mobility are hindered hence ionic conductivity decreases [19]. The ion conduction mechanism in the electrolytes may be described by the Vogel-Tammann-Fulcher (VTF) relationship which is expressed as

$$\sigma = \sigma_o \exp\left(-\frac{B}{(T - T_o)}\right) \dots\dots\dots\dots\dots\dots\dots\dots\dots\dots\dots(3)$$

where σ_o is the pre-exponential factor and T_o is the equilibrium glass transition temperature.

3.6 Dielectric Study

The study on the dielectric behavior is another study that can help in understanding the conductivity behaviour of polymer electrolytes. In this study, impedance data have been analyzed in other parameter, namely dielectric constants, ε_r. The value ε_r was determined from the equation:

$$\varepsilon_r = \frac{Z_i}{\omega C_o (Z_r^2 + Z_i^2)} \dots\dots\dots\dots\dots\dots\dots\dots\dots\dots\dots(4)$$

where C_o is vacuum capacitance. The plots of salt concentration dependence of dielectric constant at room temperature for selected frequencies are shown in Figure 8.
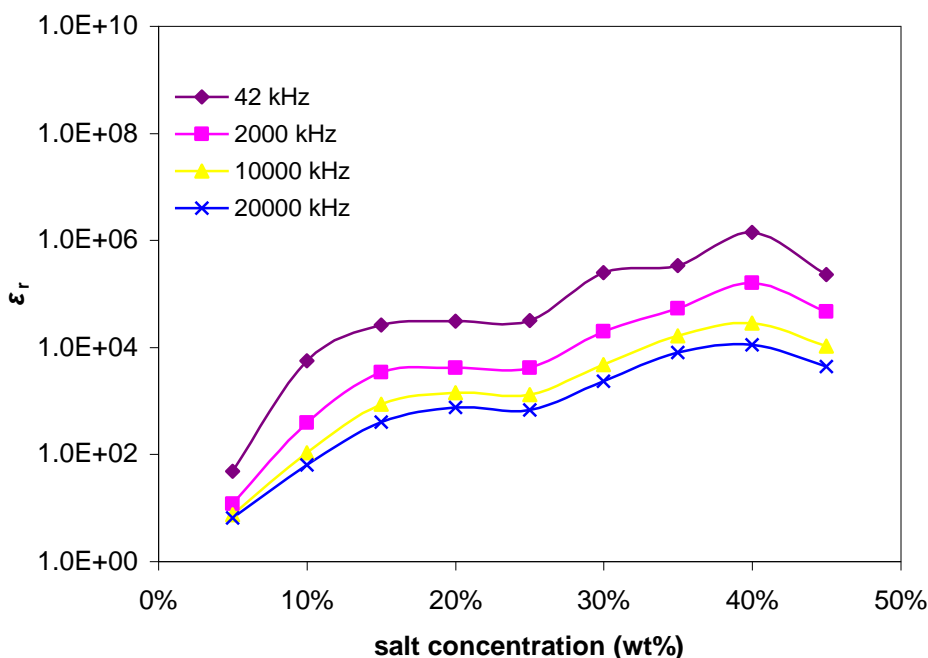
Figure 8. The plots of dielectric constant versus salt concentration at various frequencies for PVDF-HFP/PEMA–$NH_4CF_3SO_3$ system

The value of ε_r for every frequency is observed to increase with $NH_4CF_3SO_3$ salt concentration from 5 to 40 wt %. However, addition of $NH_4CF_3SO_3$ salt above 40 wt % led to a decrease in the value of ε_r. The increase in ε_r with salt concentration gives a reflection of an increase in the number of charge carriers with the increase in the salt concentration [20]. This proves that the increase in conductivity,

Figure 5, is also due to the increase in the number of the charge carriers other than the increase in the fraction of amorphous region in the electrolyte films. The decrease in the value of ε_r salt concentration above 40 wt% may be due to the decrease in density of charge carriers that is attributed to the reassociation of ions [21,22].
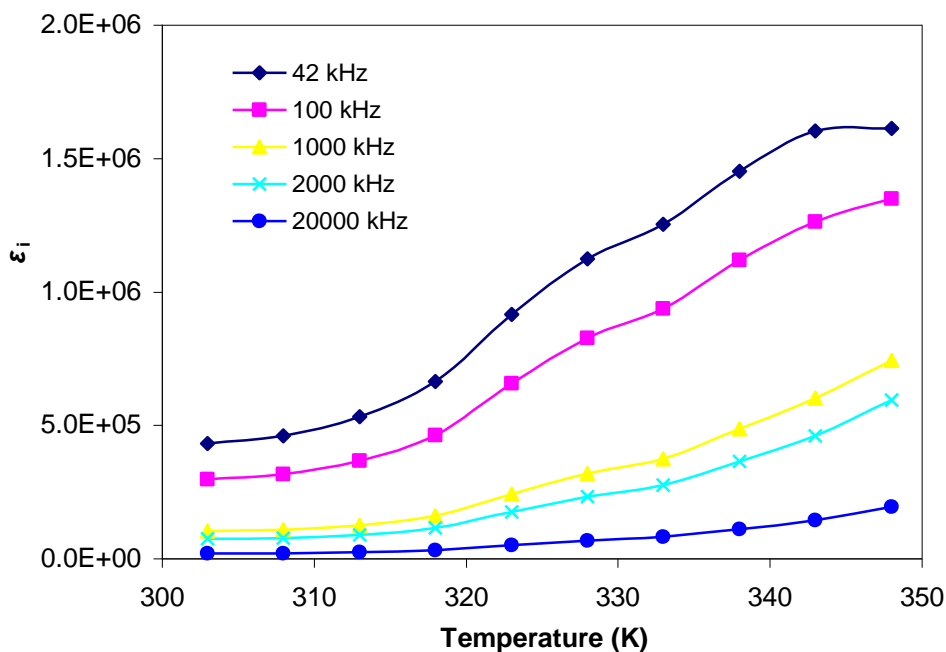
Figure 9. The plots of dielectric constant versus temperature at various frequencies for PVDF-HFP/PEMA-NH$_4$CF$_3$SO$_3$ film containing 40 wt % NH$_4$CF$_3$SO$_3$

Figure 9 shows the variations of the dielectric constant with temperature at various frequencies for polymer electrolyte containing 40 wt % of salt system. The increase in ε_r as shown in the figure is attributed to the increase in the number of charge carries. This indicates that the degree of salt dissociation is increased with the increase in temperature resulting in an increase of free charge carriers [20,23]. This also contributed to the rise in conductivity with increasing temperature as shown in Figure 8.

3.7 Transference Number Study

The ionic transference number for the electrolytes containing 30 and 40 wt % salt has been determined by the DC polarization method. The value of t_i was evaluated from the polarization current versus time plot using equation,

$$t_i = \frac{i_T - i_e}{i_T} \qquad \text{…………......………………..………..... (5)}$$

where i_T and i_e are the total and residual current respectively. Figure 10 depicts the plots of the polarization current versus time for the systems. The values of ionic transference number of the electrolytes containing 30 and 40 wt % salt are found to be 0.93 and 0.95 respectively. This suggests that the charge transport in the electrolytes was mainly ionic (protonic) [24].
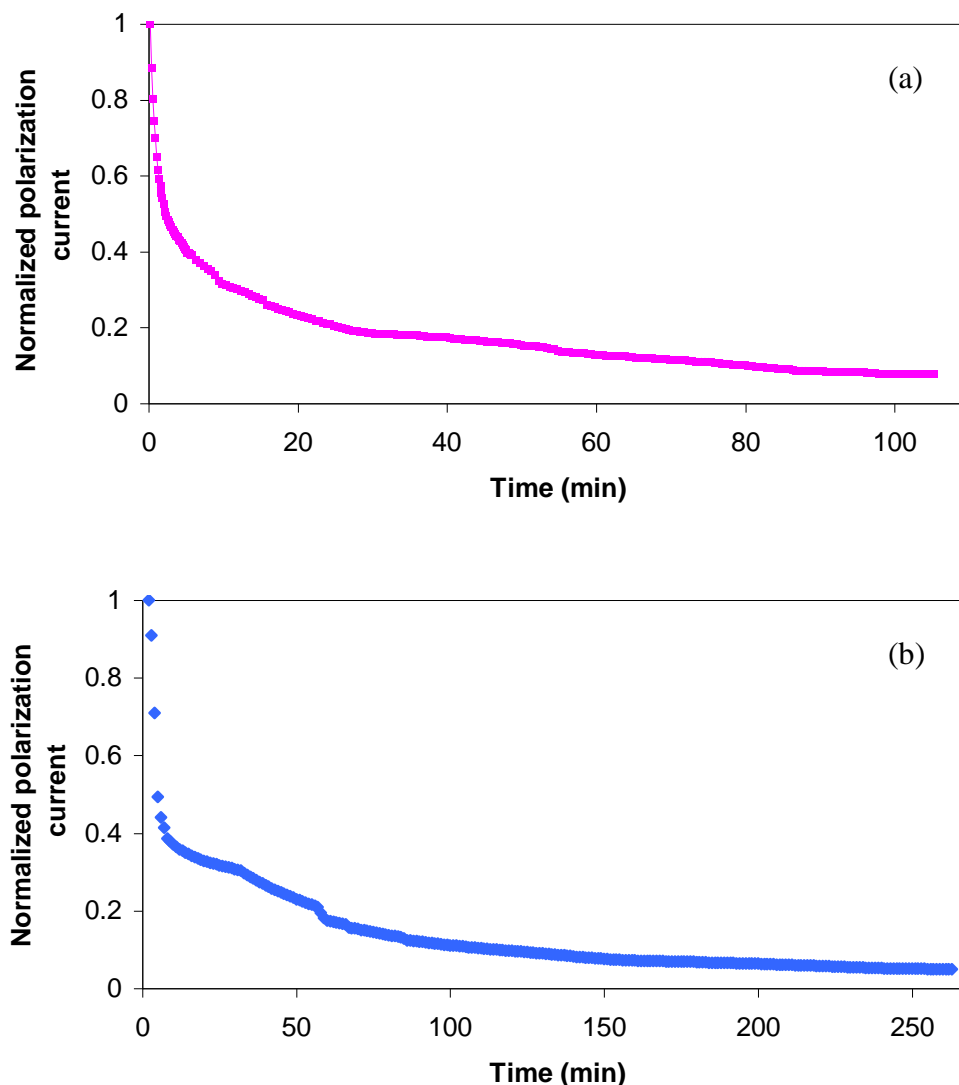
Figure 10. Variation of naormalized current with time for film PVDF-HFP/PEMA with (a) 30 and (b) 40 wt % $NH_4CF_3SO_3$

4. CONCLUSIONS

In the study, the authors have succeeded in preparing flexible free standing films of PVDf-HFP/PEMA-$NH_4CF_3SO_3$ polymer electrolytes. The XRD, SEM, DSC and dielectric constant studies showed that the conductivity of the films is influenced by the relative percentage of crystallinity and charge carrier concentration. The maximum conductivity achieved was in the order of 10^{-4} S cm^{-1} for the PVDF-HFP/PEMA containing 40 wt % of $NH_4CF_3SO_3$. Temperature dependence of conductivity of PVDF-HFP/PEMA-$NH_4CF_3SO_4$ films exhibited VTF type conductivity-temperature behavior. The

results of transference number measurements showed that the charge transport in PVDF-HFP/PEMA-NH$_4$CF$_3$SO$_3$ films was mainly due to ions (protons).

References

1. R. Baskaran, S. Selvasekarapandian, N. Kuwata, J. Kawamura, T. Hattori, *Mater. Chem. Phys.,* 98 (2006) 55.
2. M. Sivakumar, R. Subadevi, S. Rajendran, H. -C. Wu, N. -L. Wu, *European Polymer J.* 43 (2007) 4466.
3. L. Fan, Z. Dang, C. W. Nan, M. Li, *Electrochemica Acta*, 48 (2002) 205.
4. S. Ramesh, T. Winie, A. K. Arof, *European Polymer J.,* 43 (2007) 1963.
5. H. -S. Han, H. -R. Kang, S. -W. Kim, H. -T. Kim, *J. Power Sources*, 112 (2002) 461.
6. M. S. Michael, S. R. S. Prabaharan, *J. Power Sources*, 136 (2004) 408.
7. F. Wu, T. Feng, Y. Bai, C. Wu, L. Ye, Z. Feng, *Solid State Ionics,* 180 (9-10) (2009) 677.
8. E. M. Abdelrazek, *Physica B: Condensed Matter*, 400 (1-2) (2007) 26.
9. S. Ramesh, L. S. Chien, *J. Mol. Structure*, 994 (2011) 403.
10. M. Ulaganathan, S. Sundar Pethaiah, S. Rajendran, *Mater. Chem. Phys.*, 129 (2011) 471.
11. X. Tian, X. Jiang, B. Zhu, Y. Xu, *J. Membrane Sci.*, 279(1-2) (2006) 479.
12. J. -W. Choi, G. Cheruvally, Y. -H. Kim, J. -K. Kim, J. Manuel, P. Raghavan, J. -H. Ahn, K. -W. Kim, H. -J. Ahn, D. S. Choi, *Solid State Ionics*, 178(19-20) (2007) 1235.
13. M. Benz, W. B. Euler, O.J. Gregory, *Macromolecules*, 35 (2002) 2682.
14. J. -H. Cao, B. -K. Zhu, Y. -Y. Xu, *J. Membrane Sci.*, 281 (2006) 446.
15. C. S. Ramya, S. Selvasekarapandian, T. Savitha, G. Hirankumar, R. Baskaran, M.S. Bhuvaneswari, P. C. Angelo, *European Polymer J.*, 42 (2006) 2672.
16. A. Bhide, K. Hariharan, *European Polymer J.*, 43 (2007) 4253.
17. D. K. Pradhan, R. N. P. Choudhary, B. K. Samantaray, *Int. J. Electrochem. Sci.*, 3 (2008) 596.
18. N. S Mohamed, (2004). Unpublished Doctoral's thesis, Universiti Malaya, Kuala Lumpur
19. C. S. Ramya, S. Selvasekarapandian, T. Savitha, G. Hirankumar, P. C. Angelo, *Physica B: Condensed Matter*, 393 (2007) 11.
20. S. Rajendran, M. R. Prabhu, M. U. Rani, *J. Power Sources,* 180 (2008) 880.
21. M. Hema, S. Selvasekerapandian, A. Sakunthala, D. Arunkumar, H. Nithya, *Physica B: Condensen Matter*, 403 (2008) 2740.
22. G. G. Cameron, M. D. Ingram, (1989). Polymer electrolyte reviews 2 (J. R., MacCallum, C. A., Vincent,(Eds). London: Elsevier Applied Science.
23. N. Srivastava, S. Chandra, *European Polymer J.,* 36 (2000) 421.
24. M. C. R. Shastry, K.J. Rao, *Solid State Ionics*, 44 (1991) 187.
25. S. Selvasekarapandian, R. Baskaran, M. Hema. *Physica B*, 357 (2005) 412.